Experimental Analysis of Rotor-Stator interaction in a Pump-Turbine

Gabriel Dan Ciocan, Jean-Louis Kueny

Experimental Analysis of Rotor-Stator Interaction in a Pump-Turbine

Gabriel Dan CIOCAN* Institut National Polytechnique de Grenoble, France
GabrielDan.Ciocan@orange.fr
Jean Louis KUENY Institut National Polytechnique de Grenoble, France
Jean-Louis.Kueny@hmg.inpg.fr

Key words: pump-turbine, rotor-stator interaction, PIV, LDV, unsteady total pressure survey

Abstract

An exhaustive experimental exploration of the flow and pressure fields between runner and guide-vanes, of a pump-turbine, is performed using LDV, PIV and an unsteady 5 sensors probe. Measurements for design and off-design conditions, have been analyzed in both turbine and pump operation modes. For the pump operating regime, one of the investigated operating points is in the instability zone of the characteristic. This study case was used for CFD validations in the Thematic Network on Quality and Trust in the industrial applications of CFD: QNET-CFD AC6-04 test case.

Introduction

The design of pumps or turbines is mainly based on the assumption that the flow is steady in the distributor, runner and diffuser. This approach is sufficient when designing classical turbomachines. The major present requirement of the industry for compressors and gas turbines, as well as hydraulic turbines and pumps, is for more compact designs and a wide operating range. The progress in the turbomachinery design techniques allows nowadays developing new compact machines or refurbishing hydraulic devices, with a reduced rotor-stator gap. Therefore it is necessary to take into account the unsteadiness of the flow, and experimental data are of prime importance for improving our knowledge of rotor stator interaction and for calibrating new design techniques.
The optimization of pumps or turbines is now based on numerical simulation of internal flow and, in practice, the coupling between different parts of the machine must be taken into account. Several numerical techniques are now proposed for computing the flow rotor-stator interactions. The validation of these methods is only possible with detailed experiments and becomes essential, particularly for defining their validity range.

Recently, different authors analyzed the unsteady rotor-stator interaction in hydraulic machines. For instance, an experimental analysis of the runner-diffuser interaction in a pump-turbine has been performed using LDV and steady pressure survey [Ref 1]. For centrifugal pumps, many experimental methods are used. [Ref 2] analyse the tongue and impeller geometry effect from pressure measurements. [Ref 3] make an investigation on the rotor and diffuser blades for 2 different gap dimensions. [Ref 4] develop a PTV method to measure the flow in the rotor-stator region. [Ref 5] use a high-frequency response rotating five-hole probe to analyse the jet-wake flow structure in the turbine rotor. [Ref 6] use a PIV system and piezoelectric pressure transducers system to characterise the rotating stall within a centrifugal pump with a vaned diffuser. [Ref 7] make an extensive study of the rotor-stator interaction in a centrifugal pump from PIV measurements.
Simultaneously, the numerical simulation of the rotor-stator coupling is developing and a rich bibliographical background is available but it will not be detailed here. The main problems are related to the different kinds of coupling interface between the static and mobile part of the domain. The main parameters considered are the accuracy on the unsteady and turbulent quantities transmission through the interface, the calculation time and memory expenses.
This paper provides an experimental approach for characterizing the unsteady flow field in an industrial test model of pump-turbine. Both operating regimes are explored: turbine and pump. Detailed measurements are performed, for each operating regime, for 4 operating points at partial flow rate, at best efficiency and in overload conditions. In pump regime, 1 operating point is in the instability zone of the characteristic.
To characterize the rotor-stator interaction, three complementary unsteady measurement systems are employed: Laser Doppler Velocimetry, Particle Image Velocimetry and Unsteady Total Pressure Probe. Their implementation and accuracy are presented, as well as the data processing procedure. The unsteady effects of the rotor-stator interaction are quantified and analysed for both operating regimes.
The results form a data-base available for CFD validations. For the case presented in this paper, several numerical simulations have been carried-out on this test case with promising results: [Ref 8], [Ref 9], [Ref 10]. The physical behaviour is qualitatively reproduced but it is necessary to increase the accuracy of the local flow structure reproduction. It is a current challenge for the numerical simulation and these experimental data are a good tool for CFD validation.

Experimental Set-up

For this study an nq66 pump-turbine model of VATECH is employed – see Figure 1. The main geometrical characteristics can be listed as runner diameter 0.365 m, 5 rotor blades, 20 stay vanes (2 are removed for measurement accessibility raisons), 22 guide vanes and Kravatte type draft tube with a single pier.
The global measurements of flow, head and efficiency have been performed following ICE recommendations – see [Ref 11]: 0.1% precision for efficiency in the vicinity of the best efficiency point and 0.3% for the overall domain. The measurements have been performed at CREMHyG laboratory by LEGI – Turbomachines Team.

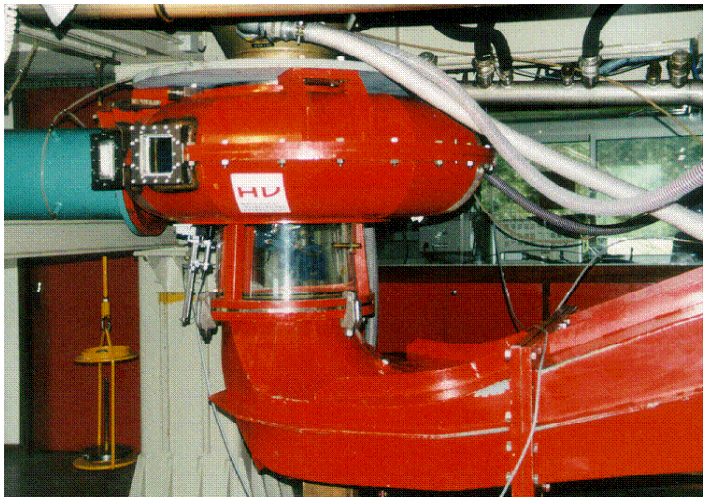

Figure 1 Pump-Turbine model

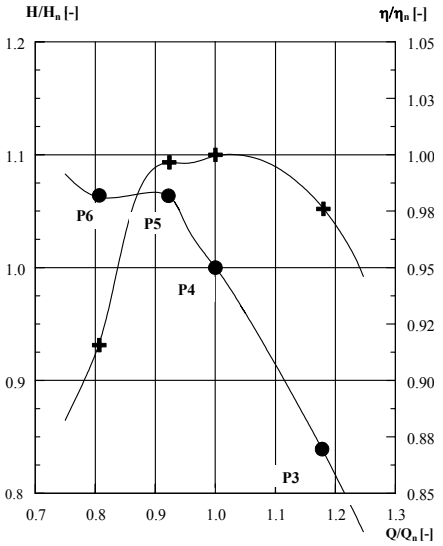

Figure 2 Operating points in pump mode

In turbine mode 4 operating points are explored, at constant guide vanes opening 18.55° – see Table 1.

Table 1 Operating points in turbine mode

No. point	T1	T2	T3	T4
Φ	.098	.114	.128	.140
Ψ	.454	.600	.753	.889

In pump mode, 4 operating points are explored – see Table 2. The operating point P6 is in the instability domain of the pump operation – see Figure 2. The measurements are performed at 1000 rpm runner rotation and 18.55° constant guide vanes opening. Tests are performed for 450 rpm and 1400 rpm as well.

Table 2 Operating points in pump mode

No. point	P6	P5	P4	P3
Φ	.100	.110	.120	.140
Ψ	.752	.756	.712	.602
Q/Qn %	.83	.92	1	1.17

Measurement Systems

The experimental tools: Laser Doppler Velocimetry, Particle Image Velocimetry and Unsteady Total Pressure Probe are used to characterize the unsteady velocity and pressure field at the rotor-stator interface and in the guide vanes channel. These three techniques are complementary: LDV for local velocity and turbulence; PIV for the velocity structure in a field and the total pressure probe for the unsteady static, total pressure and spectral analysis. A detailed description of these measurement techniques is presented in [Ref 12].

Laser Doppler Velocimetry

The LDV system is a Dantec M.T. two components system, using back-scattered light and transmission by optical fibre, with a laser of 5W Argon-Ion source. The main characteristics of the optical system are presented in Table 3.

Table 3 Optical characteristics of the laser probes

	Miniature probe	Probe for lateral components
Laser wave lengths	488 / 514.5 nm	488 / 514.5 nm
Probe diameter	14 mm	60 mm
Beam expander	30 mm	-
Beam spacing probe with expander	8 mm 14 mm	38 mm -
Focal length	100/140 mm	400 mm
Fringe spacing	~3.8 nm	~5.3 nm
Measuring volume $\sigma_X=\sigma_Y$ σ_Z	 0.15 mm 2.4 mm	 0.12 mm 2.34 mm

In order to obtain all 3 components of velocity with a 2D laser probe, a non-orthogonal arrangement is used in the runner-guide vanes gap – see Figure 3. Transparent windows with plane and parallel faces are used for the optical access. For controlling the position of the measurement volume, specific software has been developed for calculating direct and reverse light path of the laser beams through different media (air, window, water). The software is used to determine the spatial position of the laser probe for each measurement point. These calculations have been verified by CAD simulation and the probe positioning for the optical access has been optimized. The geometrical reference position of the measurements is obtained by positioning the laser beams on the window faces with accuracy better than 0.05 mm. The traversing device carrying the laser probe is attached to the spiral casing for decreasing the vibrations effects on measurements. The accuracy of the displacement relative to the device is 0.01 mm and 0.01° for angular position.

The measurement zone is a cylindrical surface parallel with the runner trailing edge for the pump operation mode - Figure 3. Tree components are measured: the tangential component of the velocity C_u, the radial component C_r and the axial component C_z.

The uncertainties of the laser measurements are estimated according to the method of Mofat and al. to 2% - [Ref 12].

Particle Image Velocimetry

The 2D instantaneous velocity field between the guide vanes is investigated with a Dantec M.T. PIV system, which consists of a double-pulsed laser, a double-frame camera and a processor unit for the acquisition synchronization and the vectors detection by cross-

correlation.

The illuminating system is composed of 2 Nd:YAG laser units, each delivering a short impulse of 9 ns and 100 mJ energy at 8 Hz frequency. The output laser beam of 532 nm is guided to a beam expander and transformed into a sheet of 1 mm width and 20° divergence.

The lighted field is visualized by a CCD camera, Kodak Megaplus ES1.0, with resolution of 1'000x1'000 pixels, from which 768x480 are used for 210x90 mm^2 investigation area. The camera lens is focused on the laser-sheet through a mirror at 45° – see Figure 4. Series of paired images at 100 µs interval are acquired synchronously with the two laser pulses. Seeding spherical particles of ~20 µm diameter, in glass covered with silver, of density equal to the water one, scatter light when excited by the laser wavelength. Their position in the measurement plane is detected on the image.

5 measurement planes are distributed on the guide vanes channel height – see Figure 4.

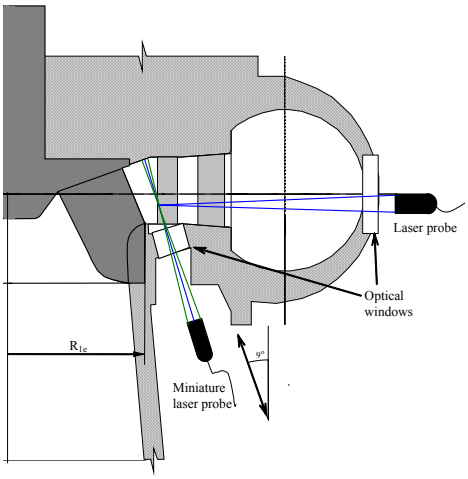

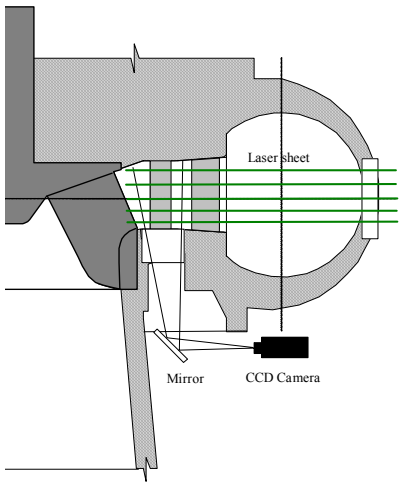

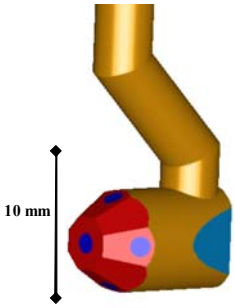

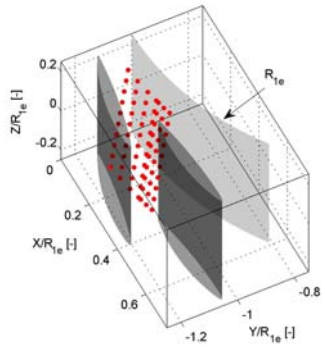

Figure 3 3D LDV measurement set-up and data points

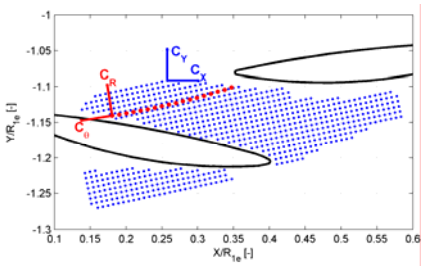

Figure 4 2D PIV measurement set-up and data points

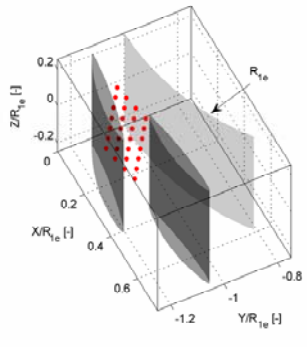

Figure 5 Unsteady total pressure probe and data points

The corresponding two-dimensional vector maps are obtained from the camera by an FFT-based algorithm. The image plane is parallel with the interfaces and the measurement plane, thus the correspondence between the image and the measurement zone is obtained via a scale factor calculated with 3 geometrical markers. The difference between the 3 scale factors calculation is less than 2% of the velocity magnitude. The accuracy of the PIV data is 3%.

Unsteady Total Pressure Survey

An unsteady total pressure probe has been developed for the high pressure part of a model of turbine or pump– see [Ref 12], [Ref 14]. Its shape is similar to the one of a 5 holes probe used for average total pressure measurements. For acceding to unsteady pressure, the probe is equipped with five ENTRAN sensors EPIH-113 placed in the probe head – see Figure 5. The probe head has a pyramidal shape and is supported by a "swan neck" tube. This design has several advantages: the pyramidal shape is recommended for the dynamic dependencies of the calibration coefficients to the Reynolds number and the rotation axis of the probe passes through the centre of mass of the sensors. The dimensions (Φ_{probe} = 7mm and $\Phi_{support}$ = 4mm) are chosen such that the flow perturbations are minimum. The sensors have been qualified for unsteady measurements and the probe has been calibrated with the hill chart technique– see [Ref 12]. This calibration technique permits to obtain reliable measurements even if the probe is not oriented in the flow direction, which is essential for unsteady flow. For the data processing, we assume that the calibration hill in the steady conditions is always valid in the unsteady conditions. This implies that the calibration results must be applied to each simultaneous pressure value and not only to the mean values. This assumption has been confirmed by the comparison between unsteady probe measurements and LDV measurements at the same location. For the results processing, 2D linear interpolation and an iterative optimization method are applied on the calibration hill. The optimization method is based on a Gauss-Newton nonlinear least-squares algorithm. The uncertainty of this technique, evaluated during the calibration is better than ~1%. However, by comparison with LDV measurements the global accuracy of the total pressure probe is 5% - see [Ref 14].
The measurement zone is similar to the LDV measurement section - see Figure 5.

Data Post-Processing

For periodic flows, the signal is reconstructed by synchronizing the acquisition with a reference signal at several time shifts. The reference signal is given by an optical encoder mounted to the runner shaft, with a resolution of 0.14°. Thus the periodic signal can be decomposed according to:

$$C_i(t) = \overline{C} + \tilde{C}(\tau) + C'(t) \qquad (1)$$

The phase-locked component $\tilde{C} + \overline{C}$ is obtained by averaging the instantaneous values C_i at the same τ value; see (3) and Figure 6.

$$\overline{C} = \langle C_i \rangle = \lim_{N\to\infty} \frac{1}{N} \sum_{i=1}^{N} C_i(t) \qquad (2)$$

$$\tilde{C}(\tau) = \lim_{N'\to\infty} \frac{1}{N'} \sum_{i=1}^{N} (C_i(\tau) - \overline{C}) \qquad (3)$$

with:

$$\tilde{\bar{C}} = 0$$
$$\langle C' \rangle = \lim_{N\to\infty}(C_i(t) - \bar{C} - \tilde{C}) = 0 \qquad (4)$$

The turbulent kinetic energy is the summation of the normal stress components. By direct measurement we obtained two orthogonal components of velocity. By the assumption that the kinetic turbulence energy is isotropic, we suppose that the three normal stress components have the same order of magnitude and the turbulent kinetic energy becomes - since the fluid is incompressible, the density will be omitted:

$$\bar{k} = \frac{3}{4}(\bar{c}_r'^2 + \bar{c}_u'^2) \qquad (5)$$

We can consider, due to the rotational periodicity that the velocity fluctuation in relation with the runner position is a deterministic phenomenon and this fluctuation does not concern the turbulent energy. So, the phase average turbulent energy becomes:

$$\tilde{k} = \frac{3}{4}(\tilde{c}_r'^2 + \tilde{c}_u'^2) \qquad (6)$$

25 phase values, equidistant in a blade to blade passage interval, T_r, are selected to complete the phase average for the LDV measurements. Thus the synchronous flow is reconstituted.

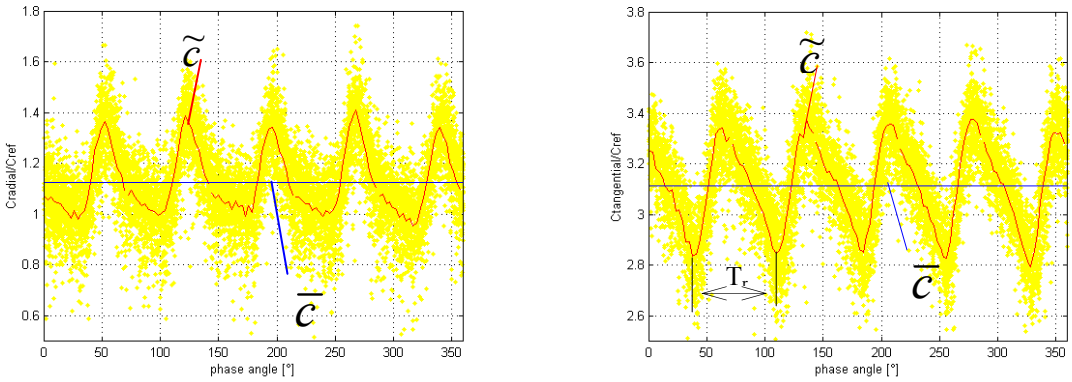

Phase radial velocity distribution *Phase tangential velocity distribution*

Figure 6 Radial and tangential velocity distribution at the turbine runner inlet

Subsequent to a mean convergence study, the mean velocity value $\bar{C}$ represents the statistic over 12´000 instantaneous velocity values.

For the PIV measurements, subsequent to a mean convergence study, the number of acquired vector maps for the mean velocity value $\bar{C}$ represents the statistic over 500 instantaneous velocity fields. The PIV acquisition is performed at constant τ value reported to the runner position.

The direct comparison between the mean velocity values, or phase average velocity values, obtained by LDV, PIV or unsteady total pressure survey measurements, shows an excellent agreement as well – see [Ref 15].

Turbine regime

In turbine regime the rotor stator-interaction is generated by the steady flow coming through the guide vanes channel and entering in the rotating frame of the runner. Additionally, the rotor blade passage in front of the guide vanes channel represents another unsteadiness source. This interaction can be described like a steady non-uniformity of the flow at the rotor inlet superposed on a secondary flow – unsteady and periodical – generated by the rotor passage. The characterization of these phenomena for the pump-turbine operating in turbine mode is presented hereafter.

Steady Analysis

The non-uniformity of the steady velocity distribution at the guide-vanes outlet represents a source of unsteadiness for the runner inlet and induces pressure fluctuations on the runner blades.

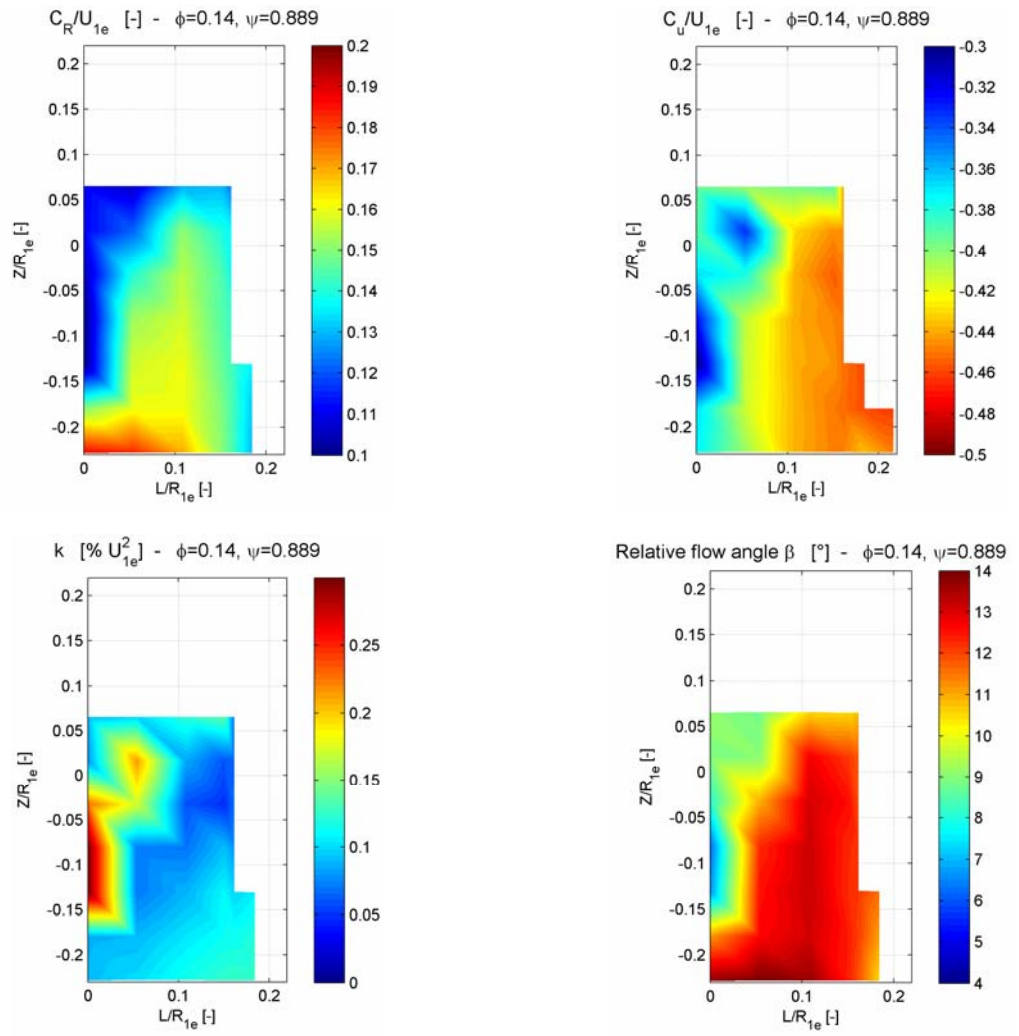

Figure 7 Steady flow – radial and tangential velocity components, k and β angle at the runner inlet

For this pump-turbine the runner inlet non-uniformity is essentially produced by two effects: the viscous wake of the guide vanes and the uneven velocity distribution in the guide vanes channel caused by potential and secondary flow effects.

The guide vanes wake is produced by the flow obstruction due to the guide vanes presence and by the pressure gradient between the guide vane pressure and suction sides. For reduced gaps between the guide vanes and the runner, the runner inlet is in the "near wake" region. As shown on Figure 7, the break-off of velocity profile in the guide vane wake is important – 40% velocity default for both velocity components (C_r and C_u) at overload operating point. The velocities are made dimensionless by:

$$U_{1e}=\omega R_{1e} \qquad (7),$$

where ω is the runner angular rotation speed. The distances: Z – channel height and L – the arc length on the measurement section are made dimensionless by R_{1e} – see Figure 3. It can be observed that in the wake zone the turbulent kinetic energy is increasing, which corresponds to the viscous wake effect. The flow is quite uniform along the channel height, without 3D effects and the C_z component has not been represented due to its small values compared to the other two.

The wake effect subsists for all operating points, with the minimum non-uniformity for the best efficiency operating point.

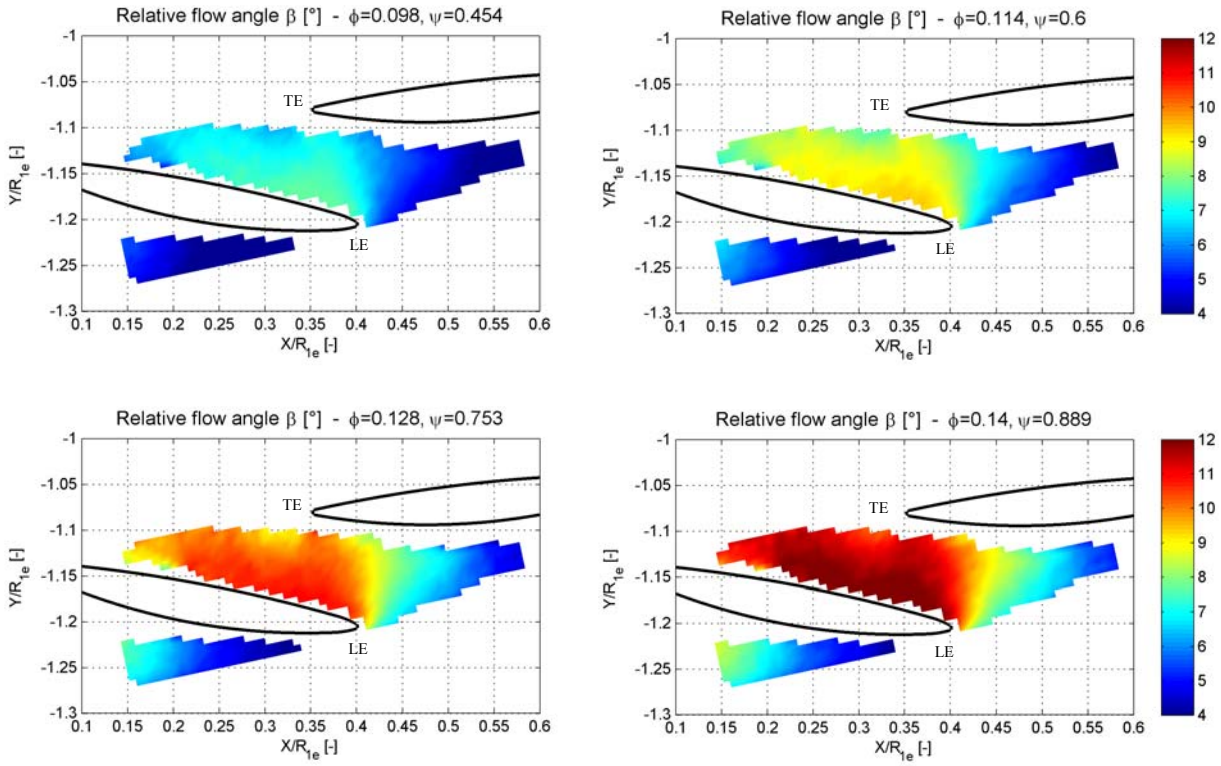

Figure 8 Relative flow angle in the guide vanes channel – half height

Concerning the turbulent kinetic energy, at the runner inlet, the difference between $\overline{k}$ and $\tilde{k}$

values, outside the wake region, is around 15%, less important for the design operating point and more important for the off-design operating points.

The second source of the non-uniformity of the velocity profile is the distribution of the velocity in the guide vanes channel. It depends on the incoming flow to the channel – spiral casing and stay vanes outlet flow, guide vanes design, operating conditions. A parameter which characterizes this evolution is the relative flow angle – β at the runner inlet, important for the runner operation. The 4 operating points are investigated for a constant guide vanes opening. However the mean β angle - Figure 8 – remains constant in the guide vanes channel for each operating point, but varies from 4° to 12° for this operating domain. The locations of the guide vane leading edge LE and trailing edge TE are represented on the figure.

Unsteady Analysis

The unsteady analysis concerns the obstruction of the guide vanes channel outlet by the runner blade passage. The runner blades pass downstream of the guide vanes channel and produce a deviation of the velocity streamlines and a local pressure increase. This blockage of the flow in the guide vane channel induces a synchronous velocity fluctuation in the entire guide vanes channel – see Figure 9. The amplitude of this fluctuation is increasing for the off-design operating points.

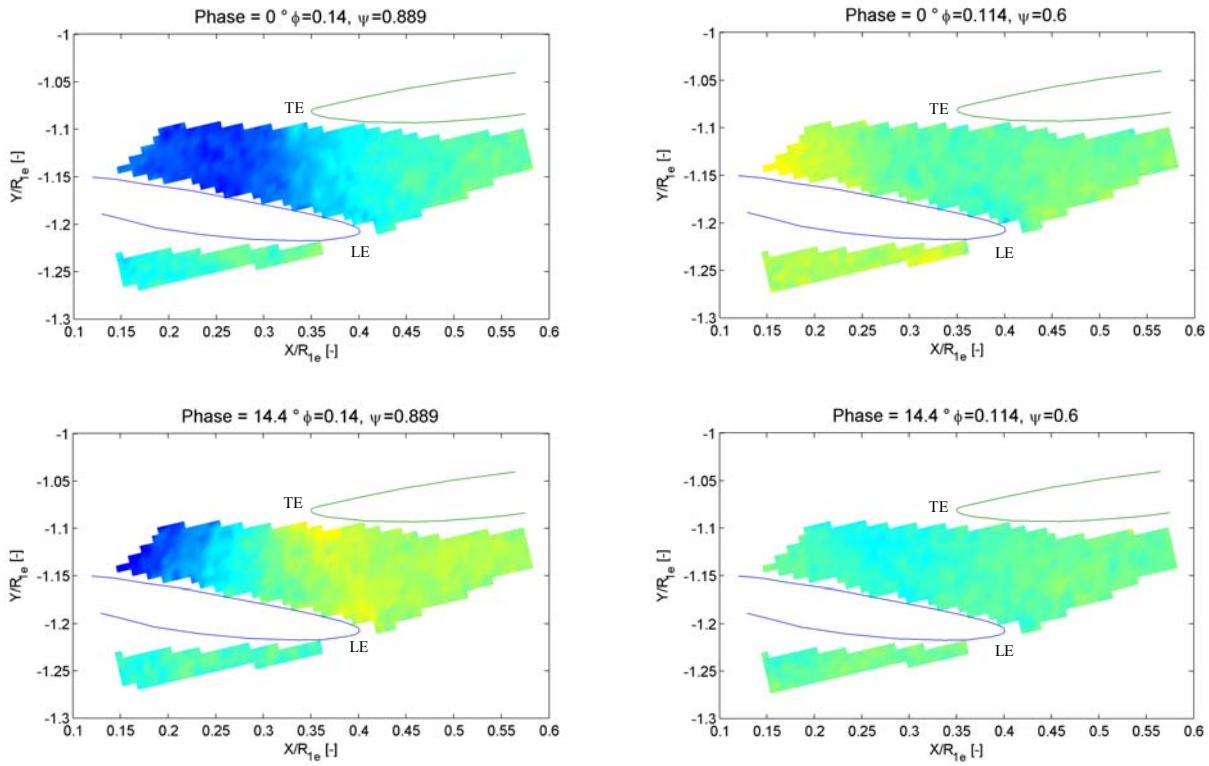

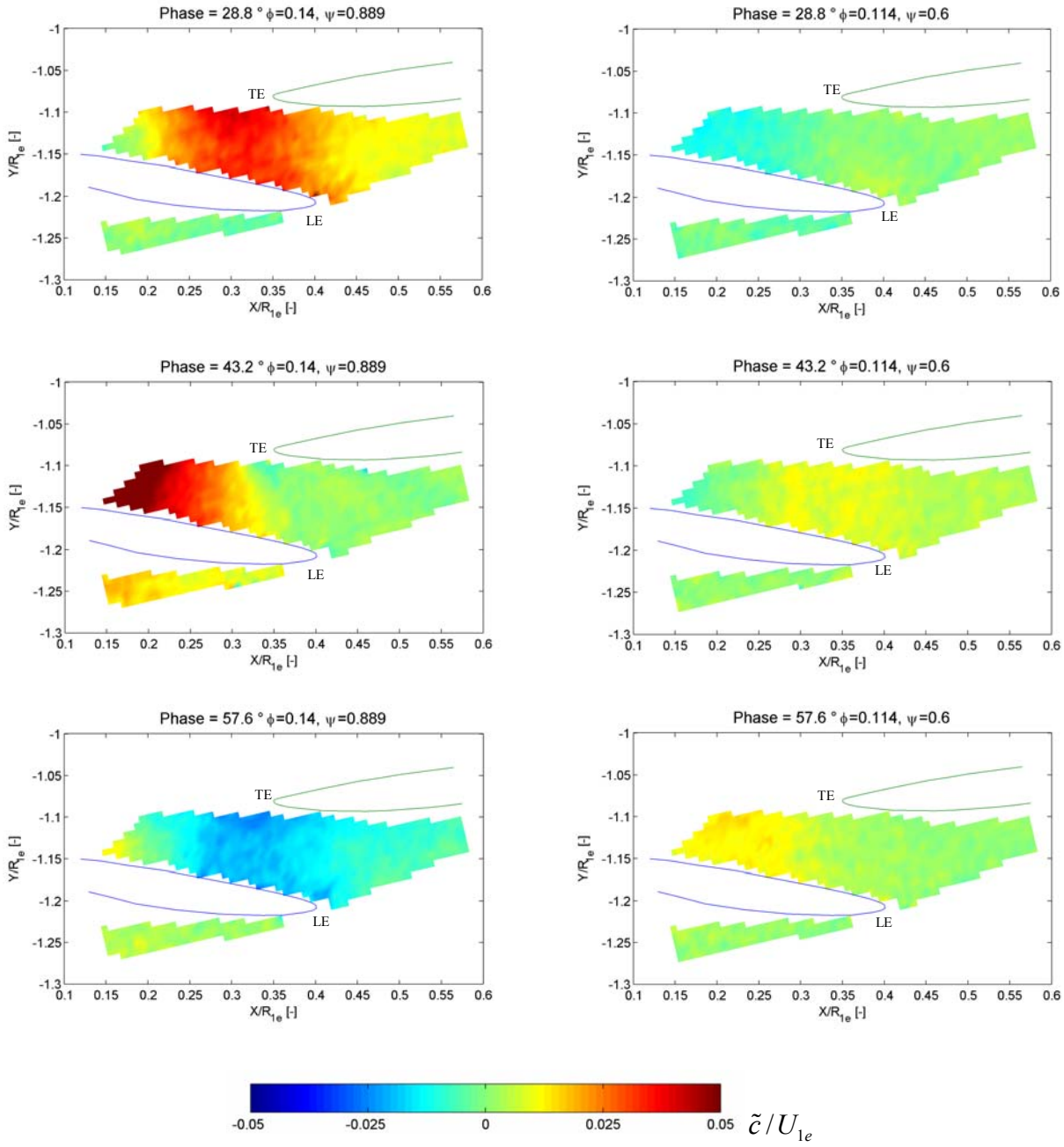

Figure 9 Unsteady velocity field in the guide vanes channel

For the runner inlet, this blockage effect provides a fluctuation of the β angle, depending on the operating point: ~4° for the φ = 0.098 and less than 1° for φ = 0.128.

Pump regime

In pump regime the flow behaviour is reversed compared to the turbine one. The steady flow distribution in the guide vanes channel is provided by the runner shroud-hub steady flow repartition. Additionally, the jet-wake velocity distribution in the runner blade to blade channel outlet represents the main unsteadiness source for the guide vanes channel.

Steady Analysis

For the steady analysis two different flow features are observed. The operating points φ = 0.110, φ = 0.120 and φ = 0.140, labelled standard operating points, present a quite similar flow behaviour. The φ = 0.100 operating point, in the instability domain of pump operation, presents different flow characteristics.

For the standard operating points, an example of the mean flow distribution is presented in Figure 10. The tangential component of the velocity has a maximum corresponding to the shroud side of the runner. This maximum is associated with a high turbulence level. The relative flow angle is quite uniform.

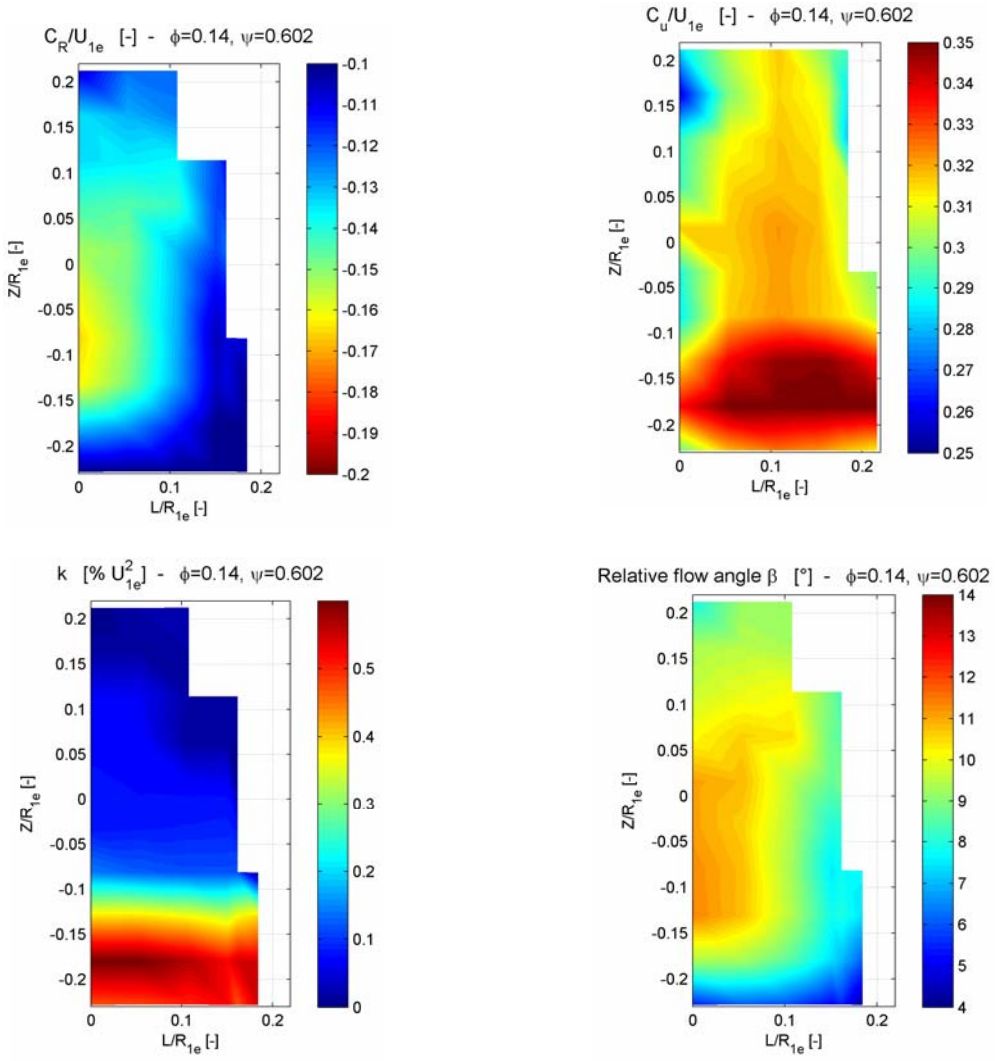

Figure 10 Steady flow – radial and tangential velocity components, k and β flow angle at the runner outlet

For the φ = 0.100 operating point, in the pump instability zone of the characteristic, it is observed that in the upper third part of the guide vanes channel, the flow is completely disorganised, and in mean value a back-flow occurs in this region – see Figure 11. In return, the mean velocity for the rest of the channel is similar to the standard operating points but the mean velocity is increased reported to the corresponding flow rate.

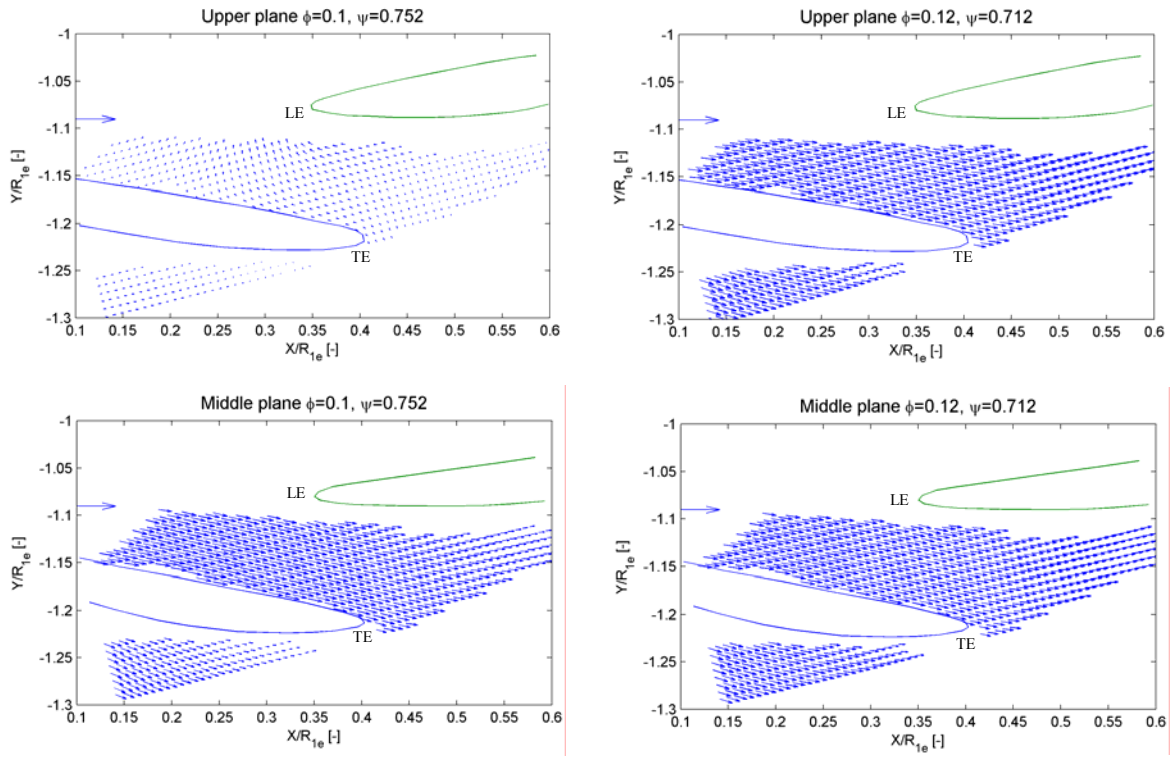

Figure 11 Mean flow velocity distribution in the guide vanes channel – pump regime

The test of the 3 runner rotation speeds shown that for this pump operation domain, the Reynolds effect can be neglected, and the similitude is respected in the measurement accuracy domain.

Unsteady Analysis

In pump mode the non-uniformity source for the guide vanes flow is the jet-wake distribution at the runner outlet. This velocity fluctuation is carried-on downstream in the guide-vanes channel, synchronously with the runner blades passage – see Figure 12. The confined guide vanes channel keeps constant the amplitude of this perturbation on its entire length. This synchronous fluctuation is present, for all operating points, in the entire height guide vane channel for all standard operating points.

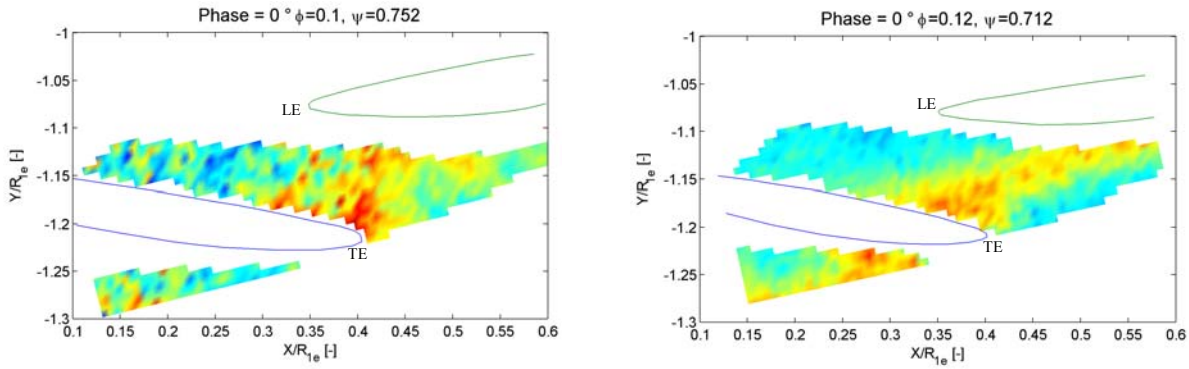

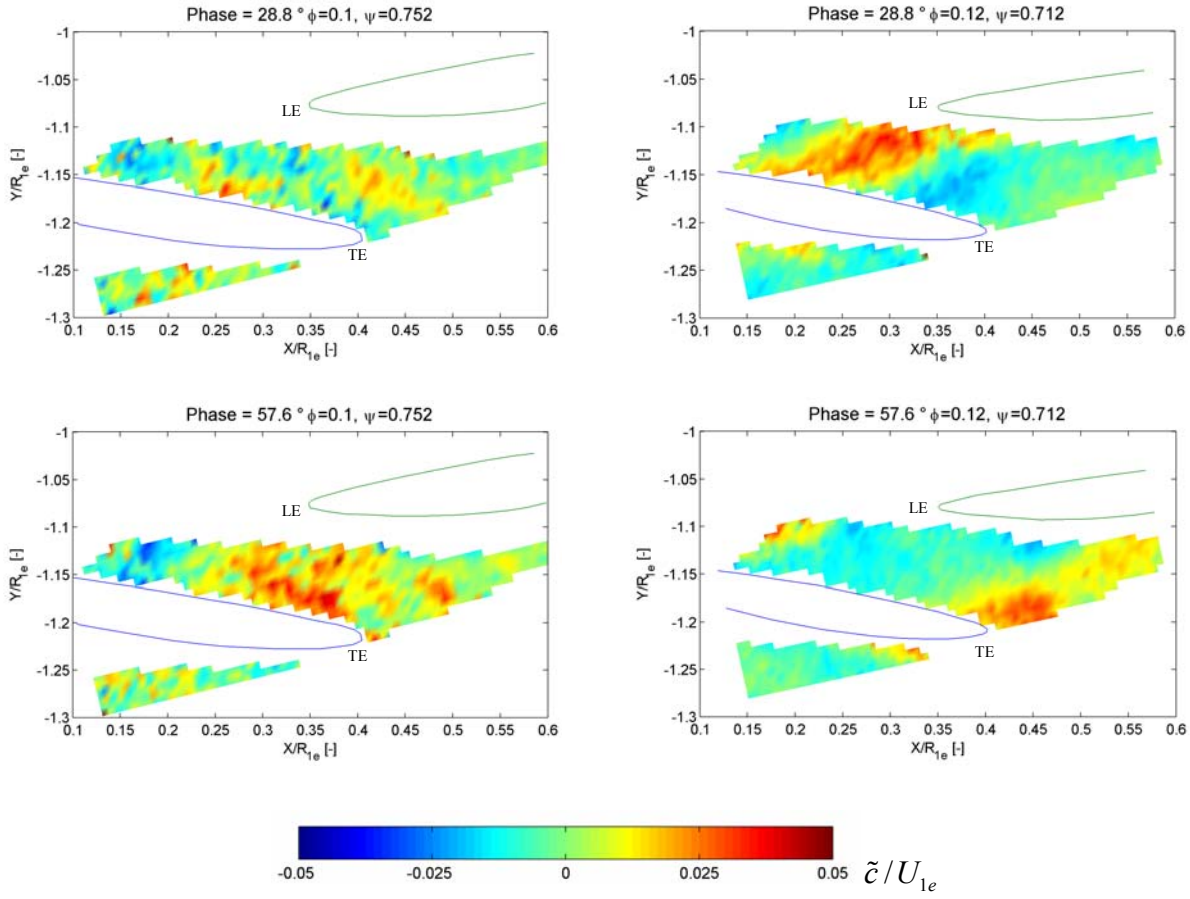

Figure 12 Runner jet-wake outlet distribution convection in the guide vanes channel

In the upper part of the guide vanes channel, for φ = 0.100, the structure of the flow is unsteady, asynchronous with the runner blade passage – see Figure 12. The flow presents instantaneous vortex releases in the main flow direction or back-flows – see the instantaneous velocity fields in Figure 13. This flow behaviour can correspond to the unsteady separation on the runner hub.

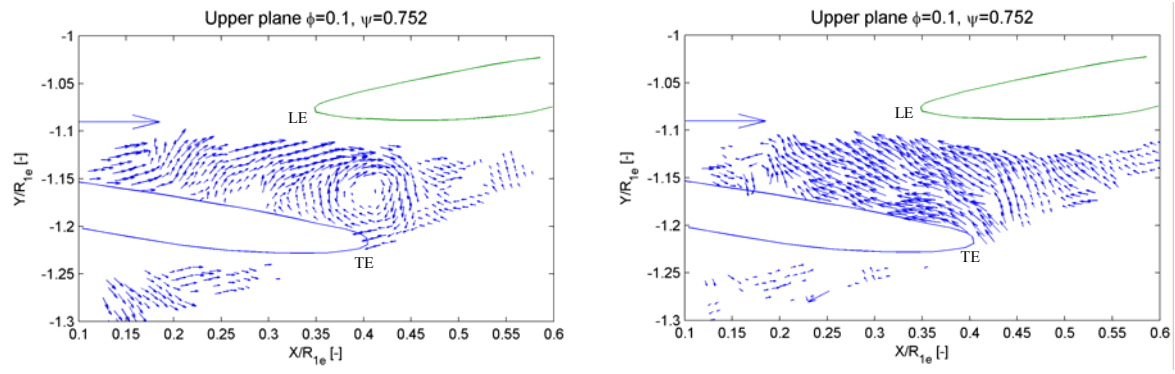

Figure 13 Instantaneous velocities fields for φ = 0.100 operating point in the upper part of the guide vanes channel

The static pressure distribution follows the velocity distribution and the main frequency amplitude is the runner blades passage $5f_n$ – see Figure 14. Other frequencies: runner passage frequency f_n, guide vanes multiplied by the runner passage $22f_n$, have small amplitudes.

The unsteady probe is unable to operate in back-flow zones. However, at the inferior limit of the back-flow region, a high amplification of the low frequencies is observed, particularly the ones lower than the blades passage frequency.

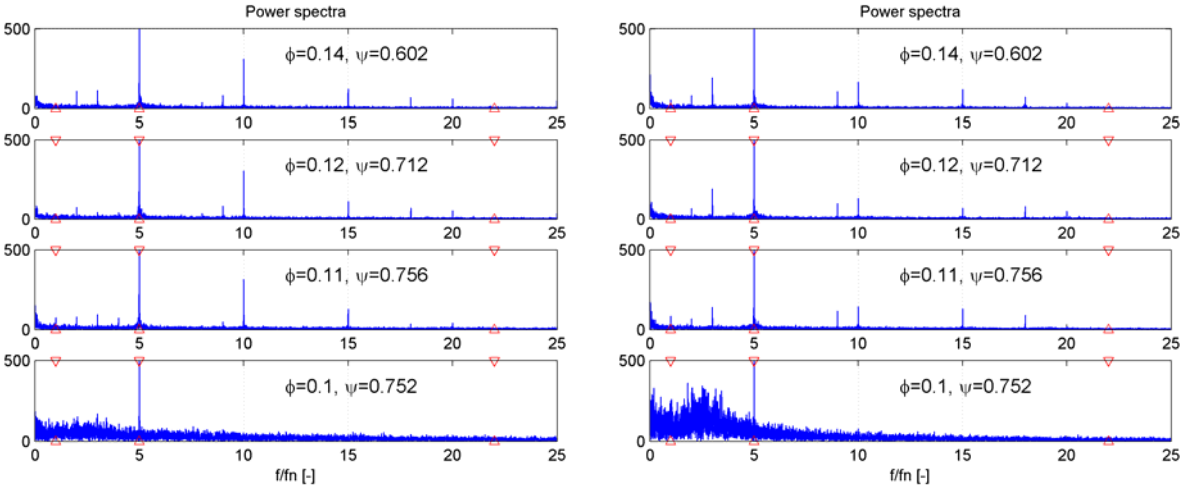

middle part of the guide vanes channel *upper part of the guide vanes channel*

Figure 14 Power spectra of total pressure signals

Conclusions

The unsteady flow between rotor and stator in a pump-turbine has been investigated using complementary types of measurements: LDV, PIV and total pressure survey. The 3D LDV measurements have a good accuracy and temporal representation in a spatial point and allow obtaining the turbulent kinetic energy. The PIV measurements provide the 2D instantaneous spatial velocity distribution and the spatial structure of the flow. The total pressure survey brings the unsteady pressure information and allows obtaining the flow characteristic frequencies by spectral analysis. The 3 types of data have been analyzed using the phase average technique synchronized with the runner rotation frequency.

The rotor-stator interaction has been quantified in both pump and turbine operating mode, for partial flow rate, best efficiency and overload operating points. In pump regime an operating point is chosen in the instability zone of the characteristic.

This case has been selected as test case for numerical calculations validation in the frame of ERCOFTAC Transition and Turbomachinery SIG's and in the Thematic Network on Quality and Trust for the industrial applications of CFD, QNET-CFD AC6 - 04 Hydraulic Pump-Turbine – [Ref 16].

Acknowledgements

The authors take this opportunity to thank CREMHyG and DANTEC Company for logistic help and the Région Rhônes-Alpes, Electricité de France and VATECH Company for their financial support for the measurements.

References

Ref 1 Ciocan, G.D., Kueny J-L., Mesquita A.A., "Steady and unsteady flow pattern between stay and guide vanes in a pump-turbine" - Proceedings of the XVIII International Symposium on

Hydraulic Machinery and Cavitation, IAHR, vol. 1, p. 381-390, Valencia, Spain, September 16-19, 1996

Ref 2 Dong R., Chu S., Katz J. "Effect of modification to tongue and impeller geometry on unsteady flow, pressure fluctuations, and noise in a centrifugal pump" Journal of Turbomachinery, vol. 119, p.506-515, 1997

Ref 3 Arndt N., Acosta A.J., Brennen C.E., Caughey T.K., "Rotor-Stator interaction in a diffuser pump", Journal of Turbomachinery, vol. 111, July 1989

Ref 4 Matsui J., Kurokawa J., Imamura H., "PTV-measurements of internal flow in a centrifugal pump of a low specific speed", FEDSM99 – 7125, Fluids Engineering Division Summer Conference, San Francisco, July 18-23, 1999

Ref 5 Liu Y.F., Lakshminarayana B., Burningham J., "Experimental investigation of the flow field in the turbine rotor passage of an automotive torque converter", FEDSM99 – 7125, Fluids Engineering Division Summer Conference, San Francisco, July 18-23, 1999

Ref 6 Sinha M., Katz J., "The onset and development of a rotating stall within a centrifugal pump with a vaned diffuser", FEDSM99 – 7198, Fluids Engineering Division Summer Conference, San Francisco, July 18-23, 1999

Ref 7 Dupont P., Caignaert G., Bois G., Schneider T., "Rotor-stator interaction in a vaned diffuser radial flow pump", FEDSM05 – 77038, Fluids Engineering Division Summer Conference, Houston, July 19-23, 2005

Ref 8 Ciocan G.D., Desvignes V., Combes J.F., Parkinson E., Kueny J-L., "Experimental and numerical analysis of rotor-stator interaction in a pump-turbine" - Proceedings of the XIX International Symposium on Hydraulic Machinery and Cavitation, IAHR, Singapore, September 9-11, 1998

Ref 9 Guedes A., Kueny J-L., Ciocan G.D., Avellan F., “Unsteady rotor-stator analysis of a hydraulic pump-turbine – CFD and experimental approach” – Proceedings of the XXI International Symposium on Hydraulic Machinery and Cavitation, IAHR, p.767-780, Lausanne, Suisse, September 9-12, 2002

Ref 10 Braun O., Kueny J-L., Avellan, F., "Numerical Analysis of Flow Phenomena related to the Unstable Energy-Discharge Characteristic of a Pump-Turbine in Pump Mode" Proceedings of ASME FEDSM2005, Fluids Engineering Division Summer Conference, Houston, TX, June 19-23, 2005

Ref 11 IEC 60193 Standard, "Hydraulic Turbines, Storage Pumps and Pump-Turbines-Model Acceptance Tests", International Electrotechnical Commission; Genève, Switzerland, 1999

Ref 12 Ciocan, G.D., "Contribution à l’analyse des écoulements 3D complexes en turbomachines", PhD Thesis, Institut National Polytechnique de Grenoble, 1998

Ref 13 Mofat, R. J., "Using Uncertainty Analysis in Planning of an Experiment", Journal of Fluid Engineering, Vol. 107 pp. 173-178, 1985

Ref 14 Ciocan G.D., Vonnez F., Baudoin J., Kueny J-L., "Unsteady five sensors probe development for hydraulic machinery" – FEDSM1998 – 5082, ASME Fluid Engineering Forum: Fluid Measurements and Instrumentation, Washington, USA, June 21-25, 1998

Ref 15 Ciocan G.D., Kueny J-L., Combes J.F., Parkinson E., "Analyse expérimentale de l'interaction roue - distributeur dans une pompe-turbine" - La Houille Blanche no. 3/4, p., Mai 22-27, 1998

Ref 16 QNET-CFD : http://www.qnet-cfd.net/